GNN for Brain Network Analysis

Group 8: DNN-X

Xuan Lin
University of California, Los Angeles
Los Angeles, CA, USA
xuanlin1991@gmail.com

Nilay Shah
University of California, Los Angeles
Los Angeles, CA, USA
nshah76@ucla.edu

Nima Zaghari
University of California, Los Angeles
Los Angeles, CA, USA
nimazaghari@gmail.com

Daisy Zheng
University of California, Los Angeles
Los Angeles, CA, USA
dayz@ucla.edu

ABSTRACT

Recognizing the associations between brain regions and specific neurological disorders remains an important objective in neuroimaging analysis. As the brain can be modeled into graphs, known as brain networks, graph neural network (GNN) models can serve as powerful tools that fit this task. However, previous models have only performed binary classification and may not be robust to different brain atlases and preprocessing techniques. With the complexity of biological data, there is a need to extend analysis to multi-class classification and validate the robustness of these models. Here we analyze a Human Connectome Project dataset via multi-class classification to supplement the existing binary classification methods. Additionally, by analyzing datasets with varying classification objectives, we further test the robustness of the model to different preprocessing workflows. We demonstrate reasonable results through our methods for multi-class classification tasks and establish the ability of the model to maintain consistency with different preprocessing techniques.

ACM Reference Format:
Xuan Lin, Nilay Shah, Nima Zaghari, and Daisy Zheng. 2021. GNN for Brain Network Analysis: Group 8: DNN-X. In *Proceedings of* . ACM, New York, NY, USA, 5 pages. https://doi.org/10.1145/nnnnnnn.nnnnnnn

1 INTRODUCTION

Consistency and interpretability are desirable objectives for any graph neural network (GNN) model, but become singularly important when performing medical image analysis. Greater transparency into a model can allow for human-intelligible interpretation thereby increasing trust in the model. Such confidence is necessary for applications in clinical settings where the decisions made based on a model's predictions have the potential to directly influence diagnostic and treatment decisions.

, ,

ACM ISBN 978-x-xxxx-xxxx-x/YY/MM…$15.00
https://doi.org/10.1145/nnnnnnn.nnnnnnn

Identifying the relationships between brain regions and specific neurological disorders remains an important goal in the fields of medicine and neuroscience. The brain can modeled as a graph, a so-called brain network, in which nodes represent regions of the brains and edges the strength of association between them. GNNs have been used to perform graph classification tasks on these brain networks, with PRGNN being a framework that identifies biomarkers for neurological disorders from functional magnetic resonance (fMRI) images. In this project, we seek to validate the agnosticity and robustness of the PRGNN framework to new datasets, methods for brain parcellation, and preprocessing pipelines.

2 PROBLEM DEFINITION

We seek to make predictions and identify salent regions that are related to the predictions through a graph neural-network architecture. To be more specific, we turn the input fMRI data into graphs that can be defined as $G = (\mathcal{V}, \mathcal{E})$. The graph G is associated with a feature set $\mathcal{H} = \{\mathbf{h}_1, ..., \mathbf{h}_N\}$ where $\mathbf{h}_i$ corresponds to the feature of node i. We also define the strength of connected edges as $e_{ij} > 0$. Our main goal is to do classification where graph neural-network make predictions. This prediction can be either the subject has certain disease, or this subject is doing a certain task (communication, motor control, etc.). In the meantime, the neural-network selects salient brain regions that are informative to the prediction task and clusters brain regions into prediction-related communities.

3 RELATED WORK

One of the main line of work in this field is based on graph convolutional and graph attention networks [12] [9]. These works propose innovative convolutional layers and pooling layers that extract the features of highly connected brain regions. They also identify the functional connectivity by assigning scores for each region to each community. Decent achievement of classification accuracy has been reported across the dataset that ranges from 70% to 90% which improves upon the benchmark algorithms such as SVM, random forest.

While there is some literature utilizing GNNs to analyze graph structured brain networks, there are some key differences with our work. For example, Li Et al. [11] presents a framework in ASD and brain subregions with task-fMRI data. Here, we augmented existing datasets with fMRI, tfMRI, and dMRI data. We believe our

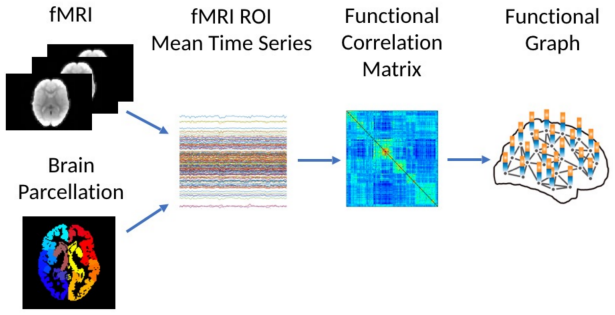

Figure 1: The designed pipeline used to process fMRI data into graphs.

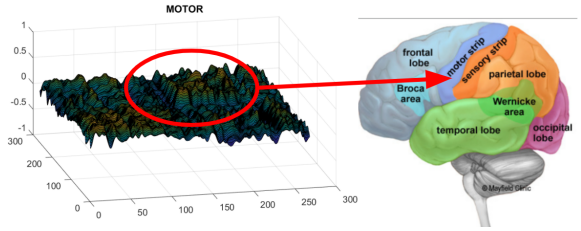

Figure 2: An example of the surf plot of a correlation matrix from HCP motor data. The peak region shows the activated regions corresponding to the motor strip in human brain.

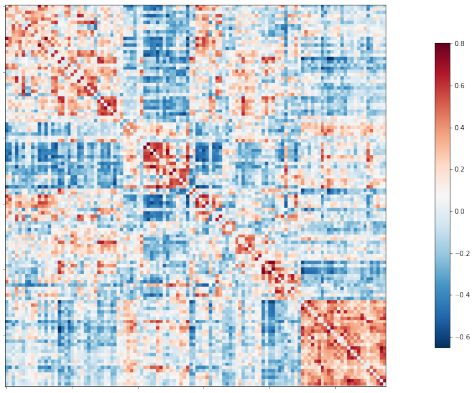

Figure 3: An example Pearson correlation matrix for an fMRI from the ABIDE dataset.

preprocessing flow and further analysis of hyperparameters lays the groundwork for future work on interpretability in evaluating a subset of nodes.

Most recent brain network analysis models utilize GNN based structures, but there has been some work that utilizes CNN-based methods. BrainNetCNN presents such an approach, with a fully convolutional neural network architecture with specially designed edge-to-edge, edge-to-node and node-to-graph filters to handle brain connectome data [7]. However, with 1.438 million trainable parameters, compared to 6 thousand used in our PRGNN based model [12], it presents a far more computationally expensive approach for brain network analysis.

4 METHODS

4.1 Data Preprocessing

Since the HCP data comes without any pre-prosessing, we need to come up with a pipeline to process the data into graphs. Figure 1 shows our designed pipeline. We parcellate the cerebral cortex into 268 regions corresponding to 268 nodes of graph using a whole-brain, functional atlas defined in a separate sample (see [17] for more details). Task functional connectivity is calculated based on the raw task time series: the mean time series of each node pair were used to calculate the Pearson correlation and partial correlation. We define a weighted undirected graph with 268 nodes per individual per task condition. The node feature are defined to be the Pearson correlation, hence the node features $h_i \in \mathbb{R}^{268}$. Edges are defined by thresholding (top 10% positive) partial correlations to achieve sparse connections. Figure 2 shows an example of the surf plot of a correlation matrix from HCP motor data. The peak region corresponding to the activated regions are where most of the edges locate.

The ABIDE data followed a similar preprocessing pipeline; however, unlike HCP, the ABIDE data was available with some preprocessing steps already done, namely normalization, timing and motion correction, and parcellation into a mean time series using the AAL functional atlas. From this data, additional preprocessing follows the same flow as descrived earlier for HCP: the Pearson correlation matrix and partial correlation matrix was calculated from the mean time series data to build a weighted graph of the brain, and then the partial correlation coefficients were used to determine the top 5% of edges to keep for the graph while the Pearson correlation coefficients acted as the node features.

5 EXPERIMENT DESIGN

5.1 Datasets

Our experimental design focused around 2 primary datasets: Autism Brain Imaging Data Exchange (ABIDE) and Human Connectome Project (HCP).

ABIDE: The ABIDE dataset looked at functional magnetic resonance imaging (fMRIs) from neurotypical individuals and individuals with Autism Spectrum Disorder (ASD). fMRI analysis is used to measure brain activity by detecting changes associated with blood flow. The goal of such analysis is to detect correlations between brain activation and a task the subject performs during the scan. The study specifically looked at 539 individuals suffering from ASD and 573 healthy control.

HCP: The HCP dataset looked at resting state fMRI (rfMRI), task-based fMRI (tfMRI), and diffusion MRI (dMRI) data from healthy individuals. rfMRI is a method of functional magnetic resonance imaging (fMRI) that is used in brain mapping to evaluate regional interactions that occur in a resting or task-negative state. Task-based fMRI is widely adopted to identify brain regions that are functionally involved in a specific task performance. dMRI is the use of specific MRI sequences as well as software that generates

images from the resulting data that uses the diffusion of water molecules to generate contrast in MR images. There were 1113 subjects in the study each presented with 7 tasks. Here we will provide a breakdown of the 7 tasks.

Gambling: This task is used to evaluate cognitive and emotional decision making. Participants play a card guessing game where money is wagered on the outcome.

Language: This task has two runs that interleave 4 blocks of a story task and 4 blocks of a math task. For the story task, Participants are presented with stories orally and are asked to recall the topic of the story. For the math task, subjects are evaluated on their response to questions about arithmetic operations.

Motor: The participants are presented with visual cues that ask them to perform a variety of exercises. For example, tapping their fingers, squeezing their toes, or move their tongue to map motor areas.

Relational: 6 different shapes are presented as stimuli to the participants. Participants are shown 2 pairs of objects at a time at the bottom and top of the screen. They have to decide what dimension differs across the objects on the top of the screen, and if the bottom objects also differ with regards to that same dimension(shape or texture).

Social: An engaging video task is presented to the subjects that is known to be a measure of social cognition. The participants make judgements on objects in a short video clip of 20 seconds.

Working Memory: Subjects read a number of sentences (usually between two and six) and tried to remember the last word of each sentence.

Emotion: The participants are presented with trials that ask them whether two faces presented on the bottom of the screen match the face at the top of the screen. They are also asked which of two shapes presented at the bottom match the top. The faces can have either angry or fearful expressions.

5.2 Network Architecture

We use the PRGNN network architecture in our model, which consists of two convolutional blocks that feed into a fully-connected readout layer, which then produces the output (Figure 4) [12]. Each graph convolutional block has a node convolutional layer which uses the graph attentional operator to update the node embeddings[16], followed by a ranking-based node pooling layer that compresses the graph to allow for lower dimensional feature extraction.

5.3 Hyperparameter Optimization

In order to streamline the process of hyperparameter optimization for different datasets and classification problems, we integrate an automated optimization framework into the model by using Optuna.

Due to the high-dimensional search space for this model, Grid Search would prove to be a naïve and exceedingly computationally expensive approach. While random search is better suited to higher dimensional search spaces, it also is expensive and does not guarantee finding the best hyperparameters. It has been shown that Gaussian-based models outperform Random Search, and thus

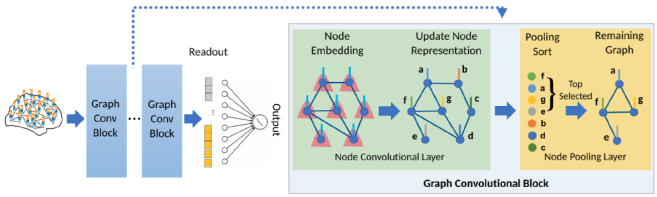

Figure 4: The PRGNN network architecture used for our model. It features two graph convolutional blocks, feeding into a fully-connect layer for output. Each graph convolutional block consists of a node convolutional layer followed by a node pooling layer.

we decided to use the TPE (Tree-structured Parzen Estimator) algorithm as our parameter sampler[3]. During each trial, for every parameter, TPE fits two Gaussian Mixture Models (GMM). One model, $l(x)$, is fit to the hyperparameter values associated with the best (smallest) loss function values, while another model $g(x)$ is fit to the remaining hyperparameter values. The algorithm thus sequentially updates its guess for every parameter by choosing the value x for each parameter that maximizes the ratio $\frac{l(x)}{g(x)}$ [4].

The hyperparameters that we tuned for our model include:

- Optimizer: the optimization algorithm to use for gradient descent (Adam, RMSProp, SGD)
- Learning Rate: the rate at which weights are updated during back-propagation
- Momentum: the momentum factor for RMSProp and SGD
- Weight-decay: an L2 regularization penalty
- Gamma: the multiplicative factor for learning rate decay
- Lambda$_{ce}$: the weight for the classification cross-entropy loss in the total loss
- Lambda$_{dist}$: the weight for the distance loss in the total loss
- Lambda$_{GLC}$: the weight for the group-level consistency loss in the total loss

The hyperparameters Lambda$_{ce}$, Lambda$_{dist}$, and Lambda$_{GLC}$ are defined in the loss function used for PRGNN:

$$L_{total} = \lambda_{ce} L_{ce} + \lambda_{dist} \sum_{l=1}^{L} L_{dist}^{(l)} + \lambda_{GLC} \sum_{c}^{C} L_{GLC}^{c}$$

The hyperparameter λ_{ce} tunes the cross-entropy loss used for the final classification prediction, the hyperparameter λ_{dist} tunes the distance loss which encourages separation between the discarded nodes and selected nodes after pooling, and the hyperparameter λ_{GLC} tunes the group-level consistency loss which adds regularization to the node importance scores calculated in the pooling layers to make them more invariant to the input.

6 EVALUATION

6.1 ABIDE Hyperparameter Choices

After running the Optuna hyperparameter tuning on our validation set for ABIDE, the following hyperparameter values were chosen for the final test evaluation:

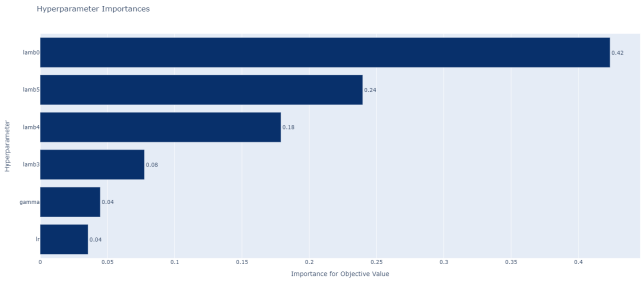

Figure 5: This graph shows the relative importance of the hyperparameters we chose to tune on the validation classification accuracy. λ_{ce} (cross-entropy, or classification, loss) is shown to have the most effect on accuracy, followed by λ_{GLC}, the consistency regularization term.

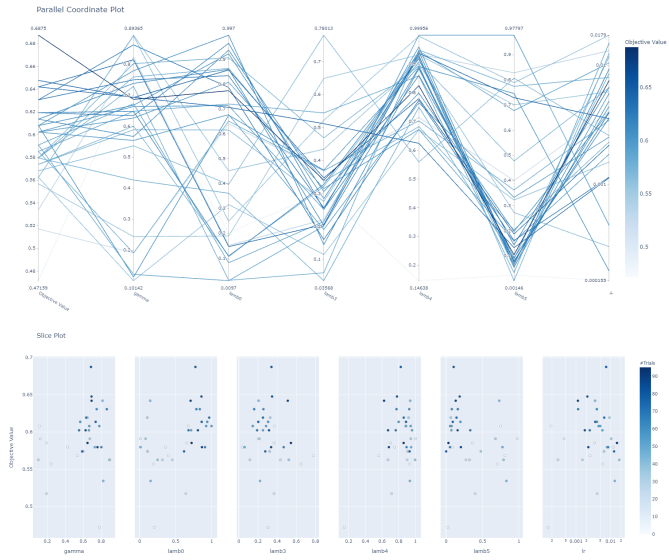

Figure 6: From the above 2 plots, it can be seen that parameter values that resulted in high accuracy scores tend to cluster in similar ranges (the absence of lines and dots at other values is also telling, as these trials tend to get pruned early on due to low accuracy and thus do not appear on these plots. For the 2 most important hyperparameters, λ_{ce} and λ_{GLC}, high values (close to 1) of λ_{ce} and low values of λ_{GLC} (close to 0) tended towards higher accuracies.

Hyperparameter	Value
Learning Rate	0.0075
Momentum	0.9
Weight Decay	0.05
γ	0.65
λ_{ce}	0.77
$\lambda_{dist}^{(1)}$	0.34
$\lambda_{dist}^{(2)}$	0.82
λ_{GLC}	0.10

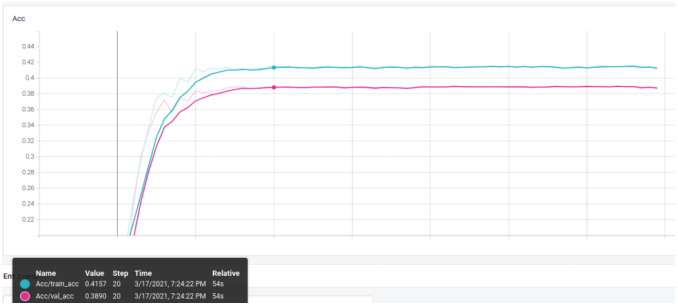

Figure 7: The Tensorboard plot from HCP dataset training reveals that the training loss converges relatively early on.

Additionally, we chose to use the Adam optimizer, Graph Attention Convolutional and TopK Pooling layers, and binary cross-entropy loss for the training process. The visualizations of the hyperparameter tuning shown in Figure 5 and 6 reveal some key insights into the optimization process.

6.2 Test Classification Accuracy

After training the model for 100 epochs, we ran the model on the test dataset that was previously set aside. The following results were obtained:

Dataset	Classification Accuracy
HCP	39%
ABIDE	63%

As mentioned earlier, the HCP dataset deals with 7-category multiclass classification, while the ABIDE dataset is used for a binary classification task. Putting the results into perspective, a "random guessing" accuracy would result in roughly 14% accuracy for HCP and a 50% accuracy for ABIDE. Comparing to this baseline, it's clear that the model is able to learn some relevant features and reasonably classify the fMRI graphs.

The confusion matrix for test classification on the ABIDE dataset is shown below. The results reveal that the model is relatively good at identifying the graphs corresponding to individuals with ASD, correctly classifying 35 out of 43 of the graphs. However, it seems overly aggressive at predicting ASD as well, classifying 15 of the 35 healthy control (HC) individuals as ASD.

	Predict HC	Predict ASD
True HC	20	15
True ASD	8	35

Overall, the results obtained from the model seem reasonable.

7 DISCUSSIONS AND CONCLUSION

7.1 Summary

The problem being studied in this paper was graph classification of fMRI scans, where fMRI images were passed through a preprocessing pipeline in order to generate the graphs. The model, originally designed for simple binary classification, was extended to be able to handle multiclass classification on the HCP dataset. We also introduced the ABIDE dataset to this problem, which acted as a new but analogous dataset for the existing binary classification

task. Further, we developed our own custom preprocessing flows for both the HCP dataset and the ABIDE dataset and used different atlases when parcellating the brain into different regions for graph generation. In this way, we evaluated the robustness of the model over new datasets, brain atlases, preprocessing flows. Finally, we integrated the optimization framework Optuna into the validation flow, allowing for easy and automated tuning of hyperparameters.

7.2 Future Work

A future direction that can be taken with this problem is to increase the interpretability of the results. One possibility is to integrate GNN-Explainer into the model evaluation flow, which can extract the specific subset of nodes that best explain the prediction made by the model. The benefit of interpretability in this problem is that it can reveal the specific brain regions that are important in determining the disease or task being studied, an important step in furthering research and diagnoses.

Ongoing work is also being done to further tune the network architecture in order to improve the performance of the model. Comparing the results with other benchmark methods should also be considered as this will provide a useful gauge of how well the model performs relative to other existing models.

REFERENCES

[1] [n.d.]. Task-fMRI 3T Imaging Protocol Details. https://protocols.humanconnectome.org/HCP/3T/task-fMRI-protocol-details.html

[2] D. M. Barch, G. C. Burgess, M. P. Harms, S. E. Petersen, B. L. Schlaggar, M. Corbetta, M. F. Glasser, S. Curtiss, S. Dixit, C. Feldt, D. Nolan, E. Bryant, T. Hartley, O. Footer, J. M. Bjork, R. Poldrack, S. Smith, H. Johansen-Berg, A. Z. Snyder, and D. C. Van Essen. 2013. Function in the human connectome: task-fMRI and individual differences in behavior. *Neuroimage* 80 (Oct 2013), 169–189.

[3] James Bergstra, Rémi Bardenet, Yoshua Bengio, and Balázs Kégl. 2011. Algorithms for Hyper-Parameter Optimization. In *Advances in Neural Information Processing Systems*, J. Shawe-Taylor, R. Zemel, P. Bartlett, F. Pereira, and K. Q. Weinberger (Eds.), Vol. 24. Curran Associates, Inc. https://proceedings.neurips.cc/paper/2011/file/86e8f7ab32cfd12577bc2619bc635690-Paper.pdf

[4] James Bergstra, Daniel Yamins, and David Cox. 2013. Making a Science of Model Search: Hyperparameter Optimization in Hundreds of Dimensions for Vision Architectures. In *Proceedings of the 30th International Conference on Machine Learning (Proceedings of Machine Learning Research, Vol. 28)*, Sanjoy Dasgupta and David McAllester (Eds.). PMLR, Atlanta, Georgia, USA, 115–123. http://proceedings.mlr.press/v28/bergstra13.html

[5] Cameron Craddock, Yassine Benhajali, Chu Carlton, Chouinard Francois, Alan Evans, András Jakab, Budhachandra Khundrakpam, John Lewis, li Qingyang, Milham Michael, Yan Chaogan, and Pierre Bellec. 2013. The Neuro Bureau Preprocessing Initiative: open sharing of preprocessed neuroimaging data and derivatives. *Frontiers in Neuroinformatics* 7 (01 2013). https://doi.org/10.3389/conf.fninf.2013.09.00041

[6] R. S. Desikan, F. Ségonne, B. Fischl, B. T. Quinn, B. C. Dickerson, D. Blacker, R. L. Buckner, A. M. Dale, R. P. Maguire, B. T. Hyman, M. S. Albert, and R. J. Killiany. 2006. An automated labeling system for subdividing the human cerebral cortex on MRI scans into gyral based regions of interest. *Neuroimage* 31, 3 (Jul 2006), 968–980.

[7] Jeremy Kawahara, Colin J. Brown, Steven P. Miller, Brian G. Booth, Vann Chau, Ruth E. Grunau, Jill G. Zwicker, and Ghassan Hamarneh. 2017. BrainNetCNN: Convolutional neural networks for brain networks; towards predicting neurodevelopment. *NeuroImage* 146 (2017), 1038–1049. https://doi.org/10.1016/j.neuroimage.2016.09.046

[8] J. Kawahara, C. J. Brown, S. P. Miller, B. G. Booth, V. Chau, R. E. Grunau, J. G. Zwicker, and G. Hamarneh. 2017. BrainNetCNN: Convolutional neural networks for brain networks; towards predicting neurodevelopment. *Neuroimage* 146 (02 2017), 1038–1049.

[9] Xiaoxiao Li and James Duncan. 2020. Braingnn: Interpretable brain graph neural network for fmri analysis. *bioRxiv* (2020).

[10] Xiaoxiao Li, Nicha C. Dvornek, Yuan Zhou, Juntang Zhuang, Pamela Ventola, and James S. Duncan. 2019. Efficient Interpretation of Deep Learning Models Using Graph Structure and Cooperative Game Theory: Application to ASD Biomarker Discovery. arXiv:1812.06181 [cs.CV]

[11] Xiaoxiao Li, Nicha C. Dvornek, Yuan Zhou, Juntang Zhuang, Pamela Ventola, and James S. Duncan. 2019. Graph Neural Network for Interpreting Task-fMRI Biomarkers. arXiv:1907.01661 [cs.LG]

[12] Xiaoxiao Li, Yuan Zhou, Nicha C Dvornek, Muhan Zhang, Juntang Zhuang, Pamela Ventola, and James S Duncan. 2020. Pooling regularized graph neural network for fmri biomarker analysis. In *International Conference on Medical Image Computing and Computer-Assisted Intervention*. Springer, 625–635.

[13] Xiaoxiao Li, Yuan Zhou, Siyuan Gao, Nicha Dvornek, Muhan Zhang, Juntang Zhuang, Shi Gu, Dustin Scheinost, Lawrence Staib, Pamela Ventola, and James Duncan. 2020. BrainGNN: Interpretable Brain Graph Neural Network for fMRI Analysis. *bioRxiv* (2020). https://doi.org/10.1101/2020.05.16.100057 arXiv:https://www.biorxiv.org/content/early/2020/05/17/2020.05.16.100057.full.pdf

[14] S. M. Smith, D. Vidaurre, C. F. Beckmann, M. F. Glasser, M. Jenkinson, K. L. Miller, T. E. Nichols, E. C. Robinson, G. Salimi-Khorshidi, M. W. Woolrich, D. M. Barch, K. Uğurbil, and D. C. Van Essen. 2013. Functional connectomics from resting-state fMRI. *Trends Cogn Sci* 17, 12 (Dec 2013), 666–682.

[15] D. C. Van Essen, K. Ugurbil, E. Auerbach, D. Barch, T. E. Behrens, R. Bucholz, A. Chang, L. Chen, M. Corbetta, S. W. Curtiss, S. Della Penna, D. Feinberg, M. F. Glasser, N. Harel, A. C. Heath, L. Larson-Prior, D. Marcus, G. Michalareas, S. Moeller, R. Oostenveld, S. E. Petersen, F. Prior, B. L. Schlaggar, S. M. Smith, A. Z. Snyder, J. Xu, and E. Yacoub. 2012. The Human Connectome Project: a data acquisition perspective. *Neuroimage* 62, 4 (Oct 2012), 2222–2231.

[16] Petar Veličković, Guillem Cucurull, Arantxa Casanova, Adriana Romero, Pietro Liò, and Yoshua Bengio. 2018. Graph Attention Networks. arXiv:1710.10903 [stat.ML]

[17] M. W. Woolrich, B. D. Ripley, M. Brady, and S. M. Smith. 2001. Temporal autocorrelation in univariate linear modeling of FMRI data. *Neuroimage* 14, 6 (Dec 2001), 1370–1386.

[18] Huzheng Yang, Xiaoxiao Li, Yifan Wu, Siyi Li, Su Lu, James S. Duncan, James C. Gee, and Shi Gu. 2019. Interpretable Multimodality Embedding Of Cerebral Cortex Using Attention Graph Network For Identifying Bipolar Disorder. *bioRxiv* (2019). https://doi.org/10.1101/671339 arXiv:https://www.biorxiv.org/content/early/2019/06/14/671339.full.pdf

[19] Rex Ying, Dylan Bourgeois, Jiaxuan You, Marinka Zitnik, and Jure Leskovec. 2019. GNNExplainer: Generating Explanations for Graph Neural Networks. arXiv:1903.03894 [cs.LG]